CHEMISTRY OF MATERIALS

pubs.acs.org/cm

Article

Mechanistic Insights into Size-Focused Growth of Indium Phosphide Nanocrystals in the Presence of Trace Water

Ajit Vikram, Arwa Zahid, Saket S. Bhargava, Logan P. Keating, Andre Sutrisno, Ankur Khare, Peter Trefonas, Moonsub Shim, and Paul J.A. Kenis*

Cite This: *Chem. Mater.* 2020, 32, 3577−3584

Read Online

ACCESS | Metrics & More | Article Recommendations | Supporting Information

ABSTRACT: Indium phosphide (InP) nanocrystals have emerged as a viable alternative to heavy metal-based colloidal quantum dots for optoelectronic applications. Traditionally, the presence of trace amounts of water during the synthesis of colloidal quantum dots is considered an undesired impurity because it prevents or slows down colloidal growth and alters the surface properties. Here, we report that fine-tuning the amount of trace water is the key for achieving size-focused growth of monodisperse InP nanocrystals synthesized using amino-phosphine precursors. Using solid-state and solution nuclear magnetic resonance, we investigated the role of trace amounts of water in surface oxidation and precursor conversion reactions. Molecular insights from UV−vis spectroscopy and NMR revealed a profound contrast between the growth rates of the nanocrystals upon the addition of water to the reaction system. We demonstrate that by addition of a specific amount of water, the reactivity of the phosphorous precursor can be tuned to enable a constant supply of monomer throughout the reaction. Under an optimal precursor conversion rate, a size-focused growth behavior that is rare for InP nanocrystals is observed, suggesting the presence of an artificial LaMer-like growth regime.

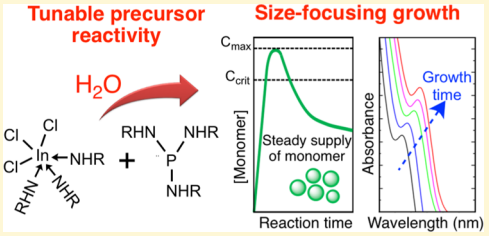

INTRODUCTION

Colloidal quantum dots (QDs) of semiconductor materials are of particular interest for applications ranging from optoelectronics and photocatalysis to bioimaging technologies because of their unique size, shape, and composition-dependent optical properties.[1−3] Among the different classes of semiconductor nanocrystals, cadmium chalcogenide-based materials have received the most attention.[4−7] The synthesis techniques developed for Cd-based materials yield highly crystalline QDs with narrow size distributions. Despite their desirable properties—high quantum yield, narrow full-width at half maximum (FWHM), and high photostability—the high toxicity of Cd-based materials remains a barrier to further commercialization.[4,8] Among various Cd-free candidates, InP QDs offer a promising alternative as a direct band gap semiconductor in the visible region.[9−11] To date, the state-of-the-art in colloidal synthesis of monodisperse InP QDs still lags behind Cd-based systems, specifically with respect to the ability to control size homogeneity during nucleation and growth.[12−16] The results of recent studies to probe the spectral linewidth of single nanocrystals confirm that the intrinsic linewidths of InP QDs are comparable to those of CdSe single nanocrystals.[17,18] Thus, the observed broad linewidths of InP QDs can be attributed primarily to particle polydispersity during synthesis. To achieve precise control over the size distribution and to improve the existing syntheses of InP QDs overall, the underlying precursor conversion, nucleation, and growth mechanisms need to be better understood.

To date, several phosphorous precursors for the synthesis of InP QDs have been reported in the literature, including tris(trimethylsilyl)phosphine (TMSP), phosphine (PH_3), aminophosphine, and magic size clusters.[18−22] TMSP and indium carboxylate-based syntheses have been most widely used to obtain monodisperse InP/ZnSe/ZnS QDs, yielding particles with emission linewidths of 40−60 nm and near-unity quantum yields.[23,24] However, the high reactivity of TMSP precursors prevents the temporal separation of precursor conversion, nucleation, and growth.[12] As a result, a large fraction of the monomer is consumed in the initial stage of the reaction, preventing sufficient monomer supply for the prolonged growth stages, which in turn limits the ability to control the size of the resulting InP QDs. Therefore, alternate precursors or synthesis approaches are needed to control the monomer delivery rates and to optimize phosphorous precursor reactivity. One such approach reported by Cossairt et al. implemented a two-phosphine strategy to tune the reactivity of silylphosphine precursors by substitution of the aryl group, such that the high reactivity of methyl precursors can be balanced with the sluggish reactivity of phenyl groups to

Received: February 22, 2020
Revised: April 1, 2020
Published: April 2, 2020

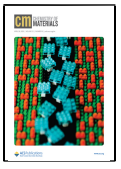

https://dx.doi.org/10.1021/acs.chemmater.0c00781
Chem. Mater. 2020, 32, 3577−3584

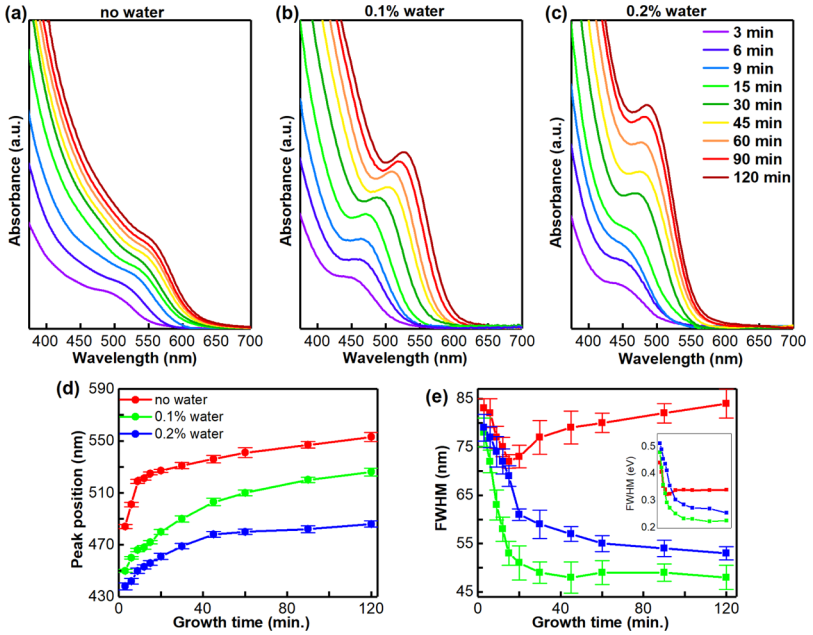

Figure 1. Evolution of the UV−vis spectra of InP QDs synthesized with addition of (a) no water, (b) 0.1% water, and (c) 0.2% water. The red shift in the absorbance peak with narrow linewidth suggests a size-focused growth behavior. The UV−vis spectra are normalized to clearly show the absorbance peak at different growth times. Absorbance peak position (d) and full-width at half maximum (e) estimated from Gaussian fitting of the UV−vis spectra for the three cases: without water addition (red), with 0.1% water addition (green), and with 0.2% water addition (blue). The inset in (e) shows the FWHM in the eV scale. All the data points represent the average of four separate InP syntheses for each case.

preserve a sufficient monomer supply throughout the QD growth stage.[14] The recent development of aminophosphine-based phosphorous precursors opens up an alternate approach as the reactivity of aminophosphine precursors is expected to be significantly lower than the reactivity of TMSP precursors.[22,25] The lower reactivity and nonpyrophoric properties of aminophosphine precursors enable an economical and easy-to-implement synthesis of InP QDs. A recent mechanistic study and subsequent optimization of the aminophosphine-based synthesis yielded InP QDs with improved (narrower) size distribution.[26] However, the ability to tune the reactivity of aminophosphine precursors to enable size-focused growth of InP QDs in a controlled manner is yet to be demonstrated.

Another critical aspect of colloidal synthesis of QDs is effective degassing of the precursors to remove trace amounts of water or other volatile species such as certain acids. Jensen et al. showed that the presence of trace water when using TMSP precursors inhibited the growth of InP QDs because of the formation of free hydroxides.[27] Mechanistic studies on *in situ* generation of water during InP synthesis revealed the formation of an alternate phosphine precursor that competes with the TMSP precursors, yielding a broad size distribution and poor reproducibility.[28] Similar work by Lee et al. using aminophosphine precursors showed that the use of hydrated indium halide species prevented nanocrystal growth after reaching an absorption peak of 485 nm in the first 3 min of growth.[29] The inhibited growth of InP QDs was hypothesized to be a direct effect of phosphate layer formation around the InP nanocrystals, thus preventing further growth of these nanocrystals.

In this work, we study the effect of adding trace amounts of water to the reaction mixture of InP QDs. We first look at how the addition of trace amounts of water affects the InP QD synthesis. Contrary to the prior literature, the presence of an optimal amount of water enables size-focused growth of InP QDs. These InP QDs grow uniformly for a prolonged time (up to 120 min) without significant oxidation of the phosphorous atoms on the surface. We then attempt to provide mechanistic insights to rationalize the role of trace amounts of water in enforcing an artificial LaMer-like growth.

RESULTS AND DISCUSSION

To study the effect of water, we first carried out a set of control experiments in the absence of added water. InP QDs were grown by injecting a room-temperature solution of tris(diethylamino)phosphine (TDEAP) precursors into a thoroughly degassed solution of indium precursors dissolved in oleylamine (OLAM) and kept at 180 °C (details provided in the Experimental Section). After precursor injection, growth of InP QDs was monitored using UV−vis spectroscopy by taking aliquots at different time intervals over 120 min (Figure 1a). The maximum in the absorption feature corresponding to the lowest energy electronic transition exhibits a red shift from 485 to 554 nm over 120 min of growth, indicating an increase in the average size of the nanocrystals. This growth is accompanied by a broadening of the absorption shoulder beyond the initial 20 min of growth, consistent with prior reports on aminophosphine-based InP synthesis.[26] Such broadening of the absorbance peak is attributed directly to the Ostwald ripening process, where the larger nanocrystals grow at the expense of the smaller nanocrystals because of the depletion of monomer supply after the initial growth of nanocrystals.

In a next set of experiments, we purposely added 0.1 and 0.2% water by volume to the flask containing the degassed solvent, followed by the injection of aminophosphine precursors to initiate QD synthesis. Growth profiles of the syntheses with addition of trace water are shown in Figure 1b,c. The red shift in the first exciton absorption peak position

https://dx.doi.org/10.1021/acs.chemmater.0c00781
Chem. Mater. 2020, 32, 3577−3584

with increasing growth time confirms the increase in the size of the InP nanocrystals during the reaction. Additionally, the absorption peak shows a blue shift with increasing water content, suggesting that the growth rate slows down upon an increase in the water content (Figure 1d). Unlike the typical case where no water was added to the reaction system, the InP QDs synthesized in the presence of added water have a well-defined absorption peak rather than a broad shoulder, thus suggesting significant improvement in the linewidth. These sharp absorption features provide a direct evidence of improved monodispersity of the nanocrystals upon addition of trace amounts of water. The absorption linewidth is quantified by estimating the absorption FWHM by fitting a mixture of Gaussian curves (n = 2−4) to the UV−vis spectra. Figure 1e compares the change in FWHM of each of the three cases: (a) no water addition, (b) 0.1% water addition, and (c) 0.2% water addition. In the control case with no added water, the FWHM shows an initial decrease from 83 nm at 3 min to 71 nm at 20 min, followed by an increase in FWHM up to 83 nm at 120 min of growth. This increase in FWHM further confirms the ripening of the nanocrystals beyond 20 min of growth. However, in the presence of trace water (both 0.1 and 0.2%), the FWHM decreases steadily to 48−55 nm while the size of the nanocrystals increases, indicating a size-focusing growth behavior. Increasing the trace amount of water to 0.4% does not yield InP QDs as evident from the absorption spectra (Figure S1, Supporting Information). Transmission electron microscopy (TEM) micrographs shown in Figure S2 show a comparison of InP QD size distribution with similar average size (absorbance peak ≈ 525 nm) synthesized without and with added water. TEM images of both samples show an average size of 2.6 and 2.5 nm with a standard deviation of 15 and 9% for particles synthesized without and with water addition, respectively. Although the quantification of size distribution using TEM technique remains challenging because of poor contrast and small size of InP QDs, size histograms obtained from TEM images (Figure S2) are consistent with narrower size distribution of particles synthesized with addition of trace water as inferred from the smaller FWHM observed in the UV−vis absorption spectra (Figure 1). Therefore, we rely on the absorption linewidth (FWHM) as a quantitative representation of the polydispersity and size distribution of the synthesized InP QDs.

Inhibition of Growth Due to Surface Oxidation. Prior to this work, Lee et al. synthesized InP QDs using hydrated indium precursors and observed no shift in the absorbance peak beyond an initial 3 min of growth.[29] The inhibited growth of InP QDs was hypothesized to be a direct result of the formation of a phosphate layer that prevents the QDs from growing beyond a certain size. In contrast, we observe continued growth, coupled with reduced FWHM up to 120 min into growth of InP QDs when controlled amounts of water are added to anhydrous In and P precursors. To further investigate the role of trace amounts of water in the oxidation of phosphorus in InP QDs, we quantified the fraction of oxidized phosphorus using solid-state ^{31}P NMR. Figure 2 shows magic angle spinning (MAS) ^{31}P NMR spectra of InP QD powders obtained through an oxygen-free purification and sample preparation inside a nitrogen-filled glovebox. The MAS rotors were modified to ensure a tight seal, preventing oxygen ingress, during data acquisition (see Experimental Section). As shown in Figure 2a, the single resonance at −200 ppm observed in the case of no water addition is attributed to

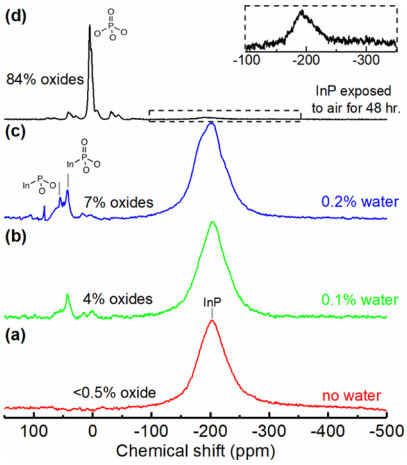

Figure 2. ^{31}P MAS SSNMR spectra of InP QDs synthesized using (a) no water addition, (b) with 0.1% water addition, and (c) 0.2% water addition during the synthesis. (d) ^{31}P MAS spectra of InP QDs exposed to air for 48 h.

nanocrystalline InP. No additional resonance corresponding to the oxidized phosphorous species is observed in this case, confirming that the aminophosphine-based synthesis used yields oxide-free InP QDs, unlike the TMSP-based synthesis, which allows significant oxidation of the surface phosphorous atoms.[30,31] Moreover, no residual oxidation is observed, even after leaving the packed rotor outside the glovebox over 24 h (Figure S3). The absence of any oxidation during postsynthesis treatment or data acquisition ensures that any observed oxidation of InP QDs can be directly attributed to the synthesis conditions only. Figure 2d shows the ^{31}P MAS spectra of a control experiment in which the synthesized InP QD powder was exposed to air for 48 h prior to acquiring NMR data. A dominant resonance appears at 5 ppm, corresponding to the completely oxidized $InPO_4$ species. Only a small, broad peak at −200 ppm for unoxidized InP is observed, indicating that nearly all phosphorous atoms present on the nanocrystal surface are oxidized. The NMR spectra shown in Figure 2b,c correspond to the InP QDs synthesized with addition of 0.1 and 0.2% water. In addition to the InP peak at −200 ppm, smaller peaks appear in the region of 17−50 ppm, which we attribute to partially oxidized phosphorous ($InPO_x$, x = 2, 3).[30] Overall, the fraction of partially or completely oxidized phosphorous remains less than 5% for syntheses in which 0.1% water was added. Assuming that 60−70% of the total phosphorous in a single nanocrystal is exposed to the surface,[32] it can be estimated that less than 10% of the surface phosphorous atoms are oxidized. Thus, extensive phosphate shells are not present around the InP nanocrystals and hence cannot prevent QD growth, contrary to the prior hypothesis in the literature.[29] The lack of a phosphate layer is also consistent with the observed increase in particle size up to 120 min of reaction time (Figure 1b,c).

Prior work by Chaudret et al. using carboxylate-based indium precursors reported a significant increase in surface oxidation from 12 to 22% upon addition of the as-synthesized InP QDs to 1.5 equivalent of water, suggesting that nearly 25−35% of all surface phosphorous species are oxidized.[30] The oxidation of phosphorous during the synthesis was attributed to *in situ* formation of water through decarboxylative coupling reaction at high temperatures. A similar extent of oxidation because of carboxylate precursors was reported by Cossairt et

https://dx.doi.org/10.1021/acs.chemmater.0c00781
Chem. Mater. 2020, 32, 3577−3584

al. using X-ray emission spectroscopy.[31] Nearly 50−85% of phosphorus species of InP/Zn(Se,S) QDs were oxidized, depending on different precursors used in the synthesis. Such high oxidation of phosphorous suggests that nearly all surface phosphorous molecules are completely oxidized, thus forming a phosphate layer around the InP core. However, recent developments in the synthesis of oxide-free InP-based nanocrystals using carboxylate-free precursors have led to the oxide-free surface but exhibiting significantly lower luminescence.[33]

Precursor Conversion Kinetics. To further identify and rationalize the role of trace amounts of water in promoting size-focused growth of the synthesized InP QDs, we monitored the reaction at the molecular level using liquid ^{31}P NMR spectroscopy. Previous reports focused on mechanistic understanding of aminophosphine chemistry and proposed a transamination reaction between aminophosphine precursors and OLAM solvent. However, the identification of the intermediate products of this transamination reaction remains ambiguous.[15,26]

Figure 3a shows the proposed reaction mechanism for the transamination reaction between TDEAP and OLAM. To identify the active phosphorous species prior to their incorporation into InP nanocrystals, a mixture of TDEAP and OLAM (without indium precursors) was degassed over 8 h at 80 °C. Solution ^{31}P NMR data of the reaction mixture showed the appearance of new intermediates/products in addition to the peak at 118 ppm (S0) corresponding to the TDEAP precursors (Figure 3). During the degassing process, the majority of the initially present S0 species is depleted slowly (decreasing peak at 118 ppm) in favor of the S3 species (peak appearing at 97 ppm) as the primary product. Three additional but less-intense resonance peaks appear, corresponding to products S1 (125 ppm), S2 (111 ppm), and S4 (12−17 ppm). Degassing the reaction mixture at a higher temperature of 180 °C also yields a nearly complete conversion of TDEAP (S0, 118 ppm) to S3 (97 ppm) as the majority product. The resonance at 97 ppm is also observed as the most intense peak for the transamination reaction when the ethyl-based aminophosphine (TDEAP) is replaced by a methyl-based aminophosphine (Figure S4). Irrespective of the nature of the alkyl group on the aminophosphine precursors, the three-fold transamination will yield an identical final product, as long as the substituting amino group (originating from OLAM) remains the same. Hence, the occurrence of the resonance at 97 ppm for both methyl and ethyl aminophosphines confirms that the peak at 97 ppm (S3) corresponds to the same fully transaminated product. Prior mechanistic investigation reported by Tessier et al. incorrectly identified the major compound at 97 ppm to be the singly transaminated product P(NHR) $(NEt_2)_2$ and the compound at 111 ppm to be doubly transaminated product $P(NHR)_2(NEt_2)$ because of their successive appearance in the reaction mixture.[15] Their hypothesis was also contradicted by Buffard et al. using a smaller amount of OLAM and methyl-based aminophosphine.[26] The species at 111 ppm was then identified to be a doubly transaminated species (S2) that is formed in important quantities upon reducing the concentration of the initial amine present in the reaction. However, when excess OLAM is present in the reaction mixture, the fully transaminated species (97 ppm) remains as the only prevalent reactive species at high temperature (Figure 3e).

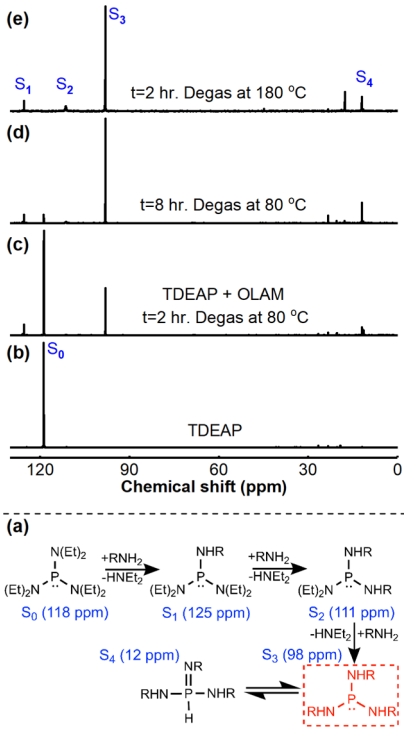

Figure 3. (a) Transamination of OLAM with TDEAP. ^{31}P liquid NMR spectra of (b) TDEAP only and (c) mixture of TDEAP and OLAM degassed for 2 and (d) 8 h at 80 °C. (e) Mixture degassed at 180 °C for 2 h. The label shown next to the NMR peaks corresponds to the labels in (a).

Upon confirmation of the fully transaminated peak at 97 ppm (S3), we attribute the additional less-intense peaks appearing at 125 and 111 ppm to the intermediate (singly or doubly) transaminated products S1 and S2, respectively (further details on the identification of the fully transaminated species are provided in the Supporting Information). The peaks observed in the 12−17 ppm region correspond to the tautomers of the transaminated products that are unreactive throughout the InP synthesis.[34] Overall, the fully transaminated product $P(NHR)_3$ (S3, 97 ppm) remains as the only prevalent reactive species responsible for the InP QD nucleation and growth. By monitoring the change in intensity of the $P(NHR)_3$ peak (S3) at 97 ppm, the precursor conversion reaction kinetics for the InP synthesis can be quantified (eq 1).

$$InCl_3 + 4P(NHR)_3 \rightarrow InP + 3P(NHR)_4Cl \quad (1)$$

Figure 4 shows the ^{31}P NMR spectra of reaction aliquots taken during the synthesis of InP QDs with different amounts of water added to the reaction mixture. In addition to the fully transaminated species S3 at 97 ppm and the unreactive tautomers S4 at 12−17 ppm, additional peaks at 30−35 ppm are observed. These correspond to the phosphonium salt, a byproduct of the InP precursor conversion reaction. For the case of synthesis without the addition of water, the fully transaminated species S3 (97 ppm) disappears completely within the first 15 min of the reaction (Figure 4a). This depletion occurs in parallel with the rapid increase in the intensity of the phosphonium salt ($P(NHR)_4Cl$) peaks in the 30−35 ppm region. This observed rapid conversion also explains the increase in linewidth of the absorbance peak beyond 20 min of growth of InP QDs synthesized without the

https://dx.doi.org/10.1021/acs.chemmater.0c00781
Chem. Mater. 2020, 32, 3577−3584

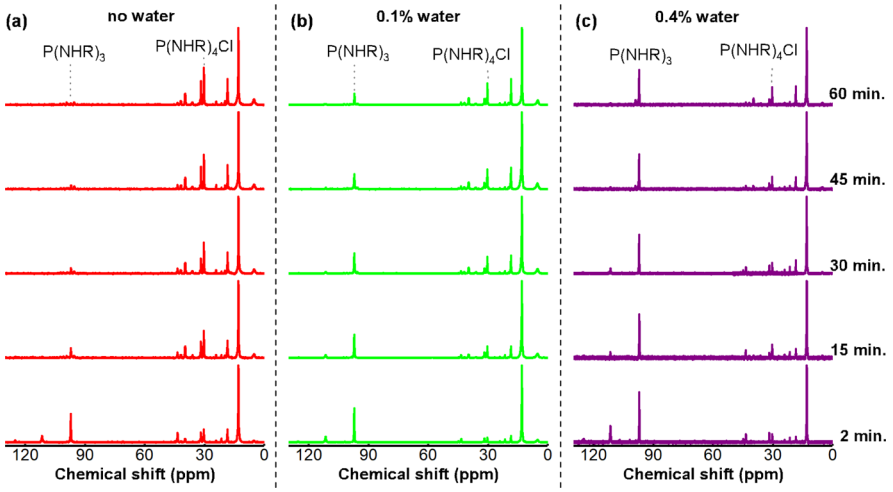

Figure 4. Kinetic study of precursor conversion reaction. ^{31}P liquid NMR spectra of reaction aliquots at different growth times for InP QDs synthesized (a) without water, (b) 0.1% water, and (c) 0.4% water. The corresponding growth time is labeled on the right side of the figure.

addition of water (Figure 1e). As the supply of reactive P-species is depleted, InP growth is driven primarily by Ostwald ripening, leading to increased polydispersity and broader linewidth.

When 0.1% water was added to the reaction mixture, no additional peaks were observed in the NMR spectra (Figure 4b), which suggests that the reaction conversion pathway remains similar with and without the addition of water. These trends are different than those observed for the TMSP precursor-based syntheses, in which the presence of protonated species yields speciation of the parent phosphorous species to form an additional phosphorous species $H_{3-n}P(SiMe_3)_n$, which leads to growth inhibition and broadening of the absorption linewidth.[28] The observation of no additional peaks in the NMR spectra when using TDEAP precursor-based synthesis confirms that no alternate phosphorous species form upon the addition of trace amounts of water. Moreover, the reactivity of the transaminated product S3 ($P(RNH)_3$) is significantly altered because of the presence of trace water. The intensity of S3 (97 ppm) decreases steadily throughout the reaction in the presence of 0.1% water (Figure 4b). The slow and steady depletion of S3 confirms that the reactivity of the phosphorous species is tuned by adding trace amounts of water. Consequently, because of the decreased precursor conversion rate, the supply of monomers remains steady throughout the reaction, thus explaining the size-focusing growth behavior of InP QDs upon addition of a specific, optimal amount of water (Figure 1). However, increasing the added amount of water to 0.4% does not lead to InP QD formation (Figure S1). The ^{31}P NMR spectra of the reaction aliquots, when 0.4% water was added to the reaction mixture, show a significantly lower rate of consumption of the transaminated phosphorous species S3, as the peak intensity at 97 ppm remains nearly steady throughout the reaction (Figure 4c). This suggests that the rate of precursor conversion in the presence of a higher amount of water is not sufficient to increase the monomer concentration above the nucleation threshold. Indeed, no distinct absorption peak is observed in the UV−vis spectra upon adding 0.4% water to the reaction mixture (Figure S1).

To substantiate this model further, we quantified the precursor conversion kinetics by monitoring the area under the peak of the 97 ppm resonance. Figure 5a shows a comparison between the three cases: (i) no water addition, (ii) optimal (0.1%) water addition, and (iii) excess (0.4%) water addition, each normalized to the concentration of the S3 species ($P(RNH)_3$) present in the aliquot taken after 2 min of reaction. For the case when no water was added, nearly 70% of the initial (at t = 2 min) species is consumed within 15 min of growth in the absence of water. An entirely different trend is observed for the synthesis upon addition of water; nearly 30 and 70% of the active P-species are still present at the end of 60 min of growth when 0.1 and 0.4% water were added, respectively. A comparison showing this clear distinction among the observed precursor conversion rate orders is visualized in Figure 5.

The trends observed in the UV−vis and NMR spectra confirm that by adjusting the trace amounts of water added to the reaction mixture, the reactivity of the active phosphorous species can be tuned significantly to artificially replicate a LaMer-like growth for InP QDs, an approach that is not feasible through standard synthesis protocols. Because the addition of trace amounts of water does not initiate formation of additional phosphorous species, we hypothesize that additional water stabilizes the InP intermediate species prior to its incorporation into the InP nanocrystals, thus lowering its reactivity and suppressing the overall precursor conversion rate (Figure 5b). $InCl_3$ as a strong Lewis acid will bind to the Lewis base present in the reaction mixture to complete its coordination chemistry that typically features a hexacoordinated indium ion.[26,35,36] When no water is added, the indium ion will be coordinated by three chlorine and three additional OLAM molecules as amine is the only stabilizing ligand present. However, in the case when both water and amine molecules are present in the reaction mixture, water behaves as an additional stabilizing ligand for the intermediate and replaces the already present amine ligand around the indium ion, and the most likely reagent is $InCl_3(H_2O)_x(RNH_2)_{3-x}$ (x = 2, 3). Similar coordination of the indium ion by a mixture of amine and water has been previously observed in the case of indium nanoparticle synthesis starting from indium chloride.[37] The butylamine ligands around the indium ion are replaced by the water molecules, either partially or fully, depending on the amount of water added. In our case, the precursor conversion reaction rate is significantly slower upon addition of water to the reaction mixture, thus suggesting that the presence of water along with amine possibly provides better stabilization, thus

https://dx.doi.org/10.1021/acs.chemmater.0c00781
Chem. Mater. 2020, 32, 3577−3584

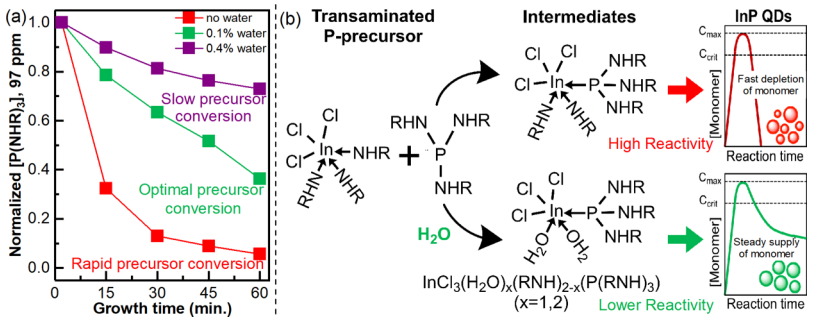

Figure 5. (a) Quantitative precursor conversion rate for three cases: (i) without water, (ii) 0.1% water, and (iii) 0.4% water, derived from the corresponding NMR spectra. Each curve is normalized to the concentration of fully transaminated product $P(NHR)_3$ at 97 ppm in Figure 4. (b) Schematic representation of the proposed hypothesis for the role of trace water in reducing the reactivity of the intermediate product, thus tuning the rate of monomer supply.

reducing the reactivity of the InP intermediate complex. Further analysis of the intermediates using density functional theory-based calculation can provide additional insight into these observed changes in the reactivity. The experimental strategy and the proposed pathway to exploit the reactivity of the aminophosphine precursors, promoting an artificial LaMer-like growth of nanocrystals, are summarized in the schematic shown in Figure 5b.

CONCLUSIONS

We have demonstrated a facile method to tune the monomer supply rate during the growth of InP nanocrystals by altering the precursor reactivity via addition of trace amounts of water. Notably, very distinct growth regimes are observed, depending on the amount of water added to the reaction mixture. ^{31}P NMR data provide mechanistic insights into the precursor conversion reaction kinetics, showing that the temporal separation of InP nucleation and growth is indeed possible by addition of a specific, optimal amount of water to the reaction mixture, thus avoiding Ostwald ripening of the nanocrystals. This results in increased monodispersity, as evident from the significantly narrower linewidth of the absorbance peaks over time. Although the resulting (unshelled) InP QDs do not exhibit any significant luminescence (QY < 1%), consistent with the prior literature, further shell growth of the ZnSe/ZnS layer around the InP core is known to drastically enhance their photoluminescence.[18] Improved monodispersity of core nanocrystals is thus expected to result in significant improvement in PL linewidth and PL QY. Coupled with recent development in the stoichiometry-controlled shell growth of ZnSe and ZnS shells on III−V QDs,[23] the size-focused growth of InP QDs demonstrated here offers the field an alternate approach to develop heavy metal-free core/shell nanocrystals for various applications. Future efforts would need to focus on further optimizing shell growth strategies to achieve high-quality InP-based core/shell nanocrystals. Moreover, our work suggests that, although the presence of trace water is traditionally considered an impurity for the colloidal synthesis of most semiconductor nanocrystals, it can be used as a critical lever to enforce LaMer-like size-focused growth of certain nanocrystals. This approach can potentially be applied successfully to other classes of nanomaterials, for example, metal phosphides that use similar aminophosphine precursors.

EXPERIMENTAL SECTION

Chemicals. Indium(III) chloride (99.999%), OLAM (technical grade, 70%), octadecene (technical grade, 90%), anhydrous ethanol (<0.005% water) and anhydrous hexane (<0.001% water), tris-(diethylamino)phosphine (97%), and tris(dimethylamino)phosphine (97%) were purchased from Sigma-Aldrich. All chemicals were degassed and stored inside the glovebox under a nitrogen environment.

Synthesis of InP QDs without Trace Water. A stock solution of dry OLAM is prepared by degassing the technical OLAM solvent at 150 °C over 2 h. Inside the glovebox, anhydrous indium(III) chloride (100 mg, 0.45 mmol) is added to the technical OLAM (5 mL, 15 mmol) in a three-necked flask. The reaction mixture is then transferred under a nitrogen atmosphere using standard Schlenk line techniques. The reaction mixture is then stirred at 500 rpm and degassed at 120 °C for 2 h through three cycles of vacuum and nitrogen purges to thoroughly remove any additional residual moisture from the flask and dissolve the reactants in the OLAM. To initiate growth, the reaction mixture is first heated under N_2 to 180 °C using a heating mantle coupled with a PID controller and thermocouple. Upon reaching a steady state of 180 °C, tris-(diethylamino)-phosphine (0.5 mL, 1.8 mmol) is quickly injected into the heated mixture (t = 0 min). Aliquots (0.1 mL) of the reaction mixture are then collected at regular intervals until t = 120 min of growth and stored under a nitrogen environment for further characterization.

Synthesis of InP QDs with Trace Water Addition. To synthesize QDs with addition of water, the same steps were carried out as explained in the previous section, except: prior to the injection of aminophosphine precursor, 0.1−0.4% of deionized water by volume (water:reaction volume) was injected into the reaction mixture at room temperature. Following the injection of water, the reaction temperature was increased to 180 °C, and the aminophosphine precursor was injected to initiate the growth of InP QDs.

Solution NMR Spectroscopy. Aliquots from the reaction mixture are taken at various time intervals and transferred to J-Young NMR tubes inside the glovebox. ^{31}P liquid NMR measurements were recorded on a Varian VXR 500 spectrometer system at the SCS NMR facility of University of Illinois at Urbana-Champaign, operating at a ^{1}H resonance frequency of 500 MHz. ^{31}P NMR spectra were referenced externally with 85% H_3PO_4.

Solid-State NMR Spectroscopy. All the ^{31}P solid-state NMR (SSNMR) experiments were conducted at 17.6 T on a Varian NMR spectrometer (VNMRS) system at the SCS NMR Facility of the University of Illinois at Urbana-Champaign, operating at a resonance frequency of $\nu 0$ (^{31}P) = 303.6 MHz at room temperature. A 4 mm Varian triple-resonance HXY T3 Narrow Bore (NB) MAS probe was used for all MAS experiments at a spinning rate of 11 kHz and ^{1}H decoupling. All samples were purified using dry ethanol and hexane, dried, packed into 4 mm O.D. zirconia rotors, and sealed with an airtight rubber spacer inside the glovebox to prevent oxidation.

https://dx.doi.org/10.1021/acs.chemmater.0c00781
Chem. Mater. 2020, 32, 3577−3584

Experimental phosphorus chemical shift referencing and pulse calibration were done using ammonium dihydrogen phosphate with a chemical shift set to 0.81 ppm. The ^{31}P 90° pulse width used was 4 μs. A calibrated recycle delay of 300 s (data not shown) was used, with a number of transients between 40 and 120 scans acquired. The NMR spectra were processed using MestReNova (version 11) processing software. Typical processing parameters for the ^{31}P solid-state NMR spectra include 100−300 Hz exponential line broadening and three zero-filling (1280 points in the time domain to 8192 points in the frequency domain).

Transmission Electron Microscopy. TEM was carried out on JEOL 2011 LaB6 TEM. For TEM sample preparation, the product was centrifuged in dry ethanol and stored inside an N_2-filled glovebox. The precipitate was dissolved in dry hexane and drop cast onto an ultrathin copper grid (EMS Diasum CF300-Cu-UL).

All postsynthesis treatments were performed under air-free conditions and using dry solvents to prevent any postsynthesis alteration of the InP QDs.

■ ASSOCIATED CONTENT

Supporting Information

The Supporting Information is available free of charge at https://pubs.acs.org/doi/10.1021/acs.chemmater.0c00781.

Additional absorbance spectra, TEM images, size distribution, SSNMR, and solution NMR for the related synthesis (PDF)

■ AUTHOR INFORMATION

Corresponding Author

Paul J.A. Kenis − *Department of Chemical and Biomolecular Engineering, University of Illinois at Urbana-Champaign, Urbana, Illinois 61801, United States;* orcid.org/0000-0001-7348-0381; Email: kenis@illinois.edu

Authors

Ajit Vikram − *Department of Chemical and Biomolecular Engineering, University of Illinois at Urbana-Champaign, Urbana, Illinois 61801, United States;* orcid.org/0000-0002-7397-3431

Arwa Zahid − *Department of Chemical and Biomolecular Engineering, University of Illinois at Urbana-Champaign, Urbana, Illinois 61801, United States*

Saket S. Bhargava − *Department of Chemical and Biomolecular Engineering, University of Illinois at Urbana-Champaign, Urbana, Illinois 61801, United States*

Logan P. Keating − *Department of Materials Science and Engineering, University of Illinois at Urbana-Champaign, Urbana, Illinois 61801, United States;* orcid.org/0000-0002-1106-9658

Andre Sutrisno − *NMR/EPR Laboratory, School of Chemical Sciences, University of Illinois at Urbana-Champaign, Urbana, Illinois 61801, United States;* orcid.org/0000-0003-2308-5708

Ankur Khare − *DuPont Electronics & Imaging, Marlborough, Massachusetts 01752, United States*

Peter Trefonas − *DuPont Electronics & Imaging, Marlborough, Massachusetts 01752, United States*

Moonsub Shim − *Department of Materials Science and Engineering, University of Illinois at Urbana-Champaign, Urbana, Illinois 61801, United States;* orcid.org/0000-0001-7781-1029

Complete contact information is available at: https://pubs.acs.org/10.1021/acs.chemmater.0c00781

Author Contributions

The manuscript was written through contributions of all the authors. All the authors have given approval to the final version of the manuscript.

Funding

This work was financially supported by DuPont Electronics & Imaging through research agreement #226772AC and an A.T. Widiger Chemical Engineering fellowship to A.V.

Notes

The authors declare no competing financial interest.

■ ACKNOWLEDGMENTS

TEM imaging was carried out in the Frederick Seitz Materials Research Laboratory Central Research Facilities, University of Illinois. NMR spectroscopy was performed at the School of Chemical Sciences NMR Lab.

■ REFERENCES

(1) Oh, N.; Kim, B. H.; Cho, S.-Y.; Nam, S.; Rogers, S. P.; Jiang, Y.; Flanagan, J. C.; Zhai, Y.; Kim, J.-H.; Lee, J.; Yu, Y.; Cho, Y. K.; Hur, G.; Zhang, J.; Trefonas, P.; Rogers, J. A.; Shim, M. Double-Heterojunction Nanorod Light-Responsive LEDs for Display Applications. *Science* **2017**, *355*, 616−619.

(2) Kagan, C. R.; Lifshitz, E.; Sargent, E. H.; Talapin, D. V. Building Devices from Colloidal Quantum Dots. *Science* **2016**, *353*, aac5523.

(3) Semonin, O. E.; Luther, J. M.; Beard, M. C. Quantum Dots for Next-Generation Photovoltaics. *Mater. Today* **2012**, *15*, 508−515.

(4) Reiss, P.; Carrière, M.; Lincheneau, C.; Vaure, L.; Tamang, S. Synthesis of Semiconductor Nanocrystals, Focusing on Nontoxic and Earth-Abundant Materials. *Chem. Rev.* **2016**, *116*, 10731−10819.

(5) Dabbousi, B. O.; Rodriguez-Viejo, J.; Mikulec, F. V.; Heine, J. R.; Mattoussi, H.; Ober, R.; Jensen, K. F.; Bawendi, M. G. (CdSe)ZnS Core−Shell Quantum Dots: Synthesis and Characterization of a Size Series of Highly Luminescent Nanocrystallites. *J. Phys. Chem. B* **1997**, *101*, 9463−9475.

(6) Murray, C. B.; Norris, D. J.; Bawendi, M. G. Synthesis and characterization of nearly monodisperse CdE (E = sulfur, selenium, tellurium) semiconductor nanocrystallites. *J. Am. Chem. Soc.* **1993**, *115*, 8706−8715.

(7) Oh, N.; Nam, S.; Zhai, Y.; Deshpande, K.; Trefonas, P.; Shim, M. Double-Heterojunction Nanorods. *Nat. Commun.* **2014**, *5*, 3642.

(8) Thomas, A.; Nair, P. V.; George Thomas, K. InP Quantum Dots: An Environmentally Friendly Material with Resonance Energy Transfer Requisites. *J. Phys. Chem. C* **2014**, *118*, 3838−3845.

(9) Dupont, D.; Tessier, M. D.; Smet, P. F.; Hens, Z. Indium Phosphide-Based Quantum Dots with Shell-Enhanced Absorption for Luminescent Down-Conversion. *Adv. Mater.* **2017**, *29*, 1700686.

(10) Mushonga, P.; Onani, M. O.; Madiehe, A. M.; Meyer, M. Indium Phosphide-Based Semiconductor Nanocrystals and Their Applications. *J. Nanomater.* **2012**, *2012*, 869284.

(11) Vikram, A.; Kumar, V.; Ramesh, U.; Balakrishnan, K.; Oh, N.; Deshpande, K.; Ewers, T.; Trefonas, P.; Shim, M.; Kenis, P. J. A. A Millifluidic Reactor System for Multistep Continuous Synthesis of InP/ZnSeS Nanoparticles. *Chemnanomat* **2018**, *4*, 943−953.

(12) Cossairt, B. M. Shining Light on Indium Phosphide Quantum Dots: Understanding the Interplay among Precursor Conversion, Nucleation, and Growth. *Chem. Mater.* **2016**, *28*, 7181−7189.

(13) Franke, D.; Harris, D. K.; Xie, L.; Jensen, K. F.; Bawendi, M. G. The Unexpected Influence of Precursor Conversion Rate in the Synthesis of III-V Quantum Dots. *Angew. Chem., Int. Ed.* **2015**, *54*, 14299−14303.

(14) Gary, D. C.; Glassy, B. A.; Cossairt, B. M. Investigation of Indium Phosphide Quantum Dot Nucleation and Growth Utilizing Triarylsilylphosphine Precursors. *Chem. Mater.* **2014**, *26*, 1734−1744.

(15) Tessier, M. D.; De Nolf, K.; Dupont, D.; Sinnaeve, D.; De Roo, J.; Hens, Z. Aminophosphines: A Double Role in the Synthesis of

Colloidal Indium Phosphide Quantum Dots. *J. Am. Chem. Soc.* **2016**, *138*, 5923−5929.
(16) Xu, Z.; Li, Y.; Li, J.; Pu, C.; Zhou, J.; Lv, L.; Peng, X. Formation of Size-Tunable and Nearly Monodisperse InP Nanocrystals: Chemical Reactions and Controlled Synthesis. *Chem. Mater.* **2019**, *31*, 5331−5341.
(17) Cui, J.; Beyler, A. P.; Marshall, L. F.; Chen, O.; Harris, D. K.; Wanger, D. D.; Brokmann, X.; Bawendi, M. G. Direct Probe of Spectral Inhomogeneity Reveals Synthetic Tunability of Single-Nanocrystal Spectral Linewidths. *Nat. Chem.* **2013**, *5*, 602−606.
(18) Tamang, S.; Lincheneau, C.; Hermans, Y.; Jeong, S.; Reiss, P. Chemistry of InP Nanocrystal Syntheses. *Chem. Mater.* **2016**, *28*, 2491−2506.
(19) Gary, D. C.; Terban, M. W.; Billinge, S. J. L.; Cossairt, B. M. Two-Step Nucleation and Growth of InP Quantum Dots Via Magic-Sized Cluster Intermediates. *Chem. Mater.* **2015**, *27*, 1432−1441.
(20) Harris, D. K.; Bawendi, M. G. Improved Precursor Chemistry for the Synthesis of III-V Quantum Dots. *J. Am. Chem. Soc.* **2012**, *134*, 20211−20213.
(21) Li, L.; Protière, M.; Reiss, P. Economic Synthesis of High Quality Inp Nanocrystals Using Calcium Phosphide as the Phosphorus Precursor. *Chem. Mater.* **2008**, *20*, 2621−2623.
(22) Tessier, M. D.; Dupont, D.; De Nolf, K.; De Roo, J.; Hens, Z. Economic and Size-Tunable Synthesis of InP/ZnE (E = S, Se) Colloidal Quantum Dots. *Chem. Mater.* **2015**, *27*, 4893−4898.
(23) Li, Y.; Hou, X.; Dai, X.; Yao, Z.; Lv, L.; Jin, Y.; Peng, X. Stoichiometry-Controlled InP-Based Quantum Dots: Synthesis, Photoluminescence, and Electroluminescence. *J. Am. Chem. Soc.* **2019**, *141*, 6448−6452.
(24) Won, Y.-H.; Cho, O.; Kim, T.; Chung, D.-Y.; Kim, T.; Chung, H.; Jang, H.; Lee, J.; Kim, D.; Jang, E. Highly Efficient and Stable InP/ZnSe/ZnS Quantum Dot Light-Emitting Diodes. *Nature* **2019**, *575*, 634−638.
(25) Kim, K.; Yoo, D.; Choi, H.; Tamang, S.; Ko, J.-H.; Kim, S.; Kim, Y.-H.; Jeong, S. Halide-Amine Co-Passivated Indium Phosphide Colloidal Quantum Dots in Tetrahedral Shape. *Angew. Chem., Int. Ed.* **2016**, *55*, 3714−3718.
(26) Buffard, A.; Dreyfuss, S.; Nadal, B.; Heuclin, H.; Xu, X.; Patriarche, G.; Mézailles, N.; Dubertret, B. Mechanistic Insight and Optimization of InP Nanocrystals Synthesized with Aminophosphines. *Chem. Mater.* **2016**, *28*, 5925−5934.
(27) Xie, L.; Harris, D. K.; Bawendi, M. G.; Jensen, K. F. Effect of Trace Water on the Growth of Indium Phosphide Quantum Dots. *Chem. Mater.* **2015**, *27*, 5058−5063.
(28) Gary, D. C.; Cossairt, B. M. Role of Acid in Precursor Conversion During InP Quantum Dot Synthesis. *Chem. Mater.* **2013**, *25*, 2463−2469.
(29) Ramasamy, P.; Kim, B.; Lee, M.-S.; Lee, J.-S. Beneficial Effects of Water in the Colloidal Synthesis of Inp/Zns Core-Shell Quantum Dots for Optoelectronic Applications. *Nanoscale* **2016**, *8*, 17159−17168.
(30) Cros-Gagneux, A.; Delpech, F.; Nayral, C.; Cornejo, A.; Coppel, Y.; Chaudret, B. Surface Chemistry of InP Quantum Dots: A Comprehensive Study. *J. Am. Chem. Soc.* **2010**, *132*, 18147−18157.
(31) Stein, J. L.; Holden, W. M.; Venkatesh, A.; Mundy, M. E.; Rossini, A. J.; Seidler, G. T.; Cossairt, B. M. Probing Surface Defects of InP Quantum Dots Using Phosphorus Kα and Kβ X-ray Emission Spectroscopy. *Chem. Mater.* **2018**, *30*, 6377−6388.
(32) Smith, A. M.; Nie, S. Semiconductor Nanocrystals: Structure, Properties, and Band Gap Engineering. *Acc. Chem. Res.* **2010**, *43*, 190−200.
(33) Tessier, M. D.; Baquero, E. A.; Dupont, D.; Grigel, V.; Bladt, E.; Bals, S.; Coppel, Y.; Hens, Z.; Nayral, C.; Delpech, F. Interfacial Oxidation and Photoluminescence of InP-Based Core/Shell Quantum Dots. *Chem. Mater.* **2018**, *30*, 6877−6883.
(34) Kolodyazhnyi, O. I.; Prinada, N. Diad Phosphorus-Nitrogen Prototropism of Tris(Alkylamino)Phosphines. *Russ. J. Gen. Chem.* **2001**, *71*, 646−647.
(35) Green, M.; Norager, S.; Moriarty, P.; Motevalli, M.; O'Brien, P. On the Synthesis and Manipulation of Inas Quantum Dots. *J. Mater. Chem.* **2000**, *10*, 1939−1943.
(36) Whitlow, S. H.; Gabe, E. J. Indium Trichloride Trihydrate Trisdioxane, Incl3.3h2o.3(C4h8o2). *Acta Crystallogr.* **1975**, *31*, 2534−2536.
(37) Dreyfuss, S.; Pradel, C.; Vendier, L.; Mallet-Ladeira, S.; Mézailles, N. The Role of Water in the Synthesis of Indium Nanoparticles. *Chem. Commun.* **2016**, *52*, 14250−14253.

https://dx.doi.org/10.1021/acs.chemmater.0c00781
Chem. Mater. 2020, 32, 3577−3584